

Supplement to: “Timing of Initial Seafloor Spreading in the Newfoundland-Iberia Rift”

Michael P. Eddy, Oliver Jagoutz, Mauricio Ibanez-Mejia

Previous Geo- and Thermochronology

Figure DR1 shows the location of all ODP drill sites that penetrated basement and/or magmatic rocks along the two studied transects. Previous geo- and thermochronology from these sites is presented in Table DR1. On the Iberian margin, sites 901, 1065, and 1067 penetrated extended continental crust and site 1069 sampled an extensional allochthon of continental crust. Sites 900 and 1068 penetrated a tectonic breccia likely involved in exhumation of the lithospheric mantle and $^{40}\text{Ar}/^{39}\text{Ar}$ plagioclase dates (Feraud et al., 1996; Jagoutz et al., 2007) and a $^{40}\text{Ar}/^{39}\text{Ar}$ hornblende date (Jagoutz et al., 2007) from these sites suggest exhumation occurred between 140 and 133 Ma (Table 1). Further oceanward, sites 897 and 899 drilled exhumed mantle capped by tectonic breccias. Minor magmatic rocks were recovered from the overlying tectonic breccia at these sites (Shipboard Scientific Party, 1994), but no radiometric dates are available. Nevertheless, the age of the first sediments overlying the mantle at ODP sites 897 and 899 is late Hauterivian to early Barremian, which provide a minimum age for mantle exhumation. The timing of magmatism and mantle exhumation at sites 1070 and 1277 is discussed within the text, and previous geo- and thermochronology results are presented in Table DR1. Site 1276 did not reach basement, but sampled alkaline basalts of ~95-105 Ma in age (Hart and Blusztajn, 2004). These sills intrude late Aptian/early Albian sediments and likely represent off-axis magmatism that occurred after lithospheric breakup.

Sample Descriptions

IB1 (13R-4 36-42) was taken from a gabbroic vein that intrudes exhumed peridotite at ODP site 1070 (Fig. DR2). The vein is almost completely altered to serpentine, talc, and chlorite with only minor relict ortho- and clinopyroxene and accessory zircon, apatite, and monazite. This mineralogy is similar to the E-MORB dike described by Beard et al. (2002). **IB2 (8R-4 11-17)** is from a gabbroic clast from the tectonic breccia that caps the basement at ODP site 1070 (Fig. DR2). It is dominantly composed of coarse (several mm) grains of moderately to severely altered albite with minor amphibole and accessory zircon, and apatite. This sample is similar to the albite clasts described by Beard et al. (2002), which Jagoutz et al. (2007) considered to represent alkaline magmas.

The exhumed peridotite at ODP site 1277 is intruded by numerous gabbroic veins (Fig. DR2). These veins are largely altered to serpentine, talc, and chlorite. Nevertheless, Muntener and Manatschal (2006) and Jagoutz et al. (2007) described two vein lithologies based on relict igneous minerals. The first is defined by the assemblage plagioclase, clinopyroxene, orthopyroxene, ilmenite, and hornblende and was considered by Jagoutz et al. (2007) to be ‘MORB-like’. **NF3 (9R-5 26-33), NF8 (9R-7 45-50), NF15 (9R-2 11-17)**, and

NF19 (9R-1 146-148) are all from highly altered (serpentine, talc, chlorite, calcite veins) gabbroic veins with all or part of this lithology. **NF8 (9R-7 45-50)** contains relict hornblende and accessory apatite and zircon and **NF15 (9R-2 11-17)** and **NF19 (9R-1 146-148)** contain relict hornblende with accessory zircon and **NF3 (9R-5 26-33)** contains highly altered pyroxenes with accessory zircon, apatite, and monazite. The second vein lithology identified by Muntener and Manatschal (2006) and Jagoutz et al. (2007) consists of phlogopite, albite, monazite, zircon, apatite, orthoamphibole, rutile, and \pm xenotime and was considered 'alkaline' by Jagoutz et al. (2007). **NF2 (9R-5 50-56)** and **NF13 (9R-4 56-64)** represent veins with this lithology and contain large relict grains of albite with accessory zircon and monazite \pm xenotime. The location of each gabbroic vein is shown in Fig. DR2.

U-Pb Zircon Geochronology Methods

Gabbroic veins within ODP cores 1070 and 1277 were crushed using a mortar and pestle and zircons were separated from this material using standard methods. U-Pb dates were produced using chemical abrasion- isotope dilution- thermal ionization mass spectrometry (CA-ID-TIMS) using methods slightly modified from Mattinson (2005) and outlined in Appendix A of Eddy et al. (2016). All of the isotopic measurements were made on the VG Sector 54 or Isotopx X62 thermal ionization mass spectrometers (TIMS) at the Massachusetts Institute of Technology and are presented in Table DR2. Samples were spiked with the EARTHTIME ^{202}Pb - ^{205}Pb - ^{233}U - ^{235}U isotopic tracer (Condon et al., 2015; McLean et al., 2015), which permits correction for both Pb and U fractionation using the tracer's known $^{202}\text{Pb}/^{205}\text{Pb}$ and $^{233}\text{U}/^{235}\text{U}$ ratios. We corrected for interferences under masses 202, 204, and 205 by measuring 201 and 203, assuming that they represent $^{202}\text{BaPO}_4$ and ^{203}Tl , and using natural isotopic abundances to correct for $^{202}\text{BaPO}_4$, $^{204}\text{BaPO}_4$, $^{205}\text{BaPO}_4$, and ^{205}Tl . We assume that zircon does not include any initial common Pb (Pb_c) during crystallization and that all measured ^{204}Pb is from laboratory contamination. We corrected for this contamination using the procedures outlined in McLean et al. (2011) and a laboratory Pb_c isotopic composition of $^{206}\text{Pb}/^{204}\text{Pb} = 18.145833 \pm 0.475155$ (1σ abs.), $^{207}\text{Pb}/^{204}\text{Pb} = 15.303903 \pm 0.295535$ (1σ abs.), and $^{208}\text{Pb}/^{204}\text{Pb} = 37.107788 \pm 0.875051$ (1σ abs.), calculated from 149 procedural blanks measured in the MIT isotope geochemistry lab between 2009 and 2015. The mass of Pb_c measured in our analyses is comparable to those seen in total procedural blanks and supports the assumption that zircon does not include Pb_c during crystallization. Initial secular disequilibrium in the ^{238}U - ^{206}Pb decay system occurs due to exclusion of Th during zircon crystallization (Scharer, 1984). We corrected for this disequilibrium using the calculated $[\text{Th}/\text{U}]_{\text{zircon}}$ and a $[\text{Th}/\text{U}]_{\text{magma}} = 3.2$ based on the average MORB composition presented by Gale et al. (2013) and an arbitrary uncertainty of ± 1 (2σ). Data reduction was done with the U-Pb_Redux software package (Bowring et al., 2011) and used the decay constants for ^{235}U and ^{238}U presented in Jaffey et al. (1971). All isotopic ratios are presented in Table DR2 and shown as concordia plots in Fig. DR3. Rank order plots of Th-corrected $^{206}\text{Pb}/^{238}\text{U}$ dates are shown for both ODP sites 1070 and 1277 in Fig. DR4.

All dates in Table 1 represent weighted means of Th-corrected $^{206}\text{Pb}/^{238}\text{U}$ dates. We used the mean square of weighted deviates (MSWD) to assess whether the spread in dates from individual zircons represented real age dispersion (MSWD $\gg 1$) or could be attributed to analytical uncertainty. Only NF2 contained a zircon that was demonstrably older than the main population. This zircon (z6) is discordant (Fig. DR3) and may contain an inherited core. The presence of a xenocrystic core in this sample would provide further evidence for the exhumed mantle at ODP site 1277 to be lithospheric in origin (e.g., Muntener and Manatschal, 2006). However, in order to preserve as much material for U-Pb analysis as possible, the zircons used in this study were not imaged and we cannot conclusively say whether or not this grain contained a core.

Hf Isotopic Measurements

Trace element aliquots were collected from all dated zircons using the methods of Schoene et al. (2010). These aliquots were dried down to chloride salts, converted to 200 μl of 1 M HCl- 0.1M HF and split into two new aliquots: 30 μl for trace element analysis and 170 μl for Hf isotopic measurement. Hf was purified from the 170 μl aliquot using AG50W-X8 cation resin following methods slightly modified from Goodge and Vervoort (2006) to minimize isobaric interferences to ^{176}Hf caused by ^{176}Lu and ^{176}Yb . Our elution scheme is very similar to that presented in Goodge and Vervoort (2006) and uses micro-columns holding ca. 100 μl of un-used, pre-cleaned, and equilibrated AG50W-X8 resin. After column chemistry, approximately 450 μl of 1 M HCl- 0.1M HF were added to the purified Hf cut in order to bring the volume of each aliquot up to ~ 1.2 ml, and the Hf isotopic composition of the purified solutions was measured on a Nu Plasma II-ES multi collector-inductively coupled plasma-mass spectrometer (MC-ICP-MS) at the MIT Department of Earth, Atmospheric, and Planetary Sciences. All Hf isotopic data is presented in Table DR3. Repeat runs of JMC-475 standard solution at 25 ppb concentration were measured in order to monitor instrument stability, determine the reproducibility of the measured ratios, and adjust the obtained values for instrumental bias. Two or three measurements of JMC-475 were conducted every 8 or 10 unknowns during our analytical sessions, and unknowns were corrected using a standard-sample bracketing approach. External reproducibility for any given set of unknowns was estimated as the 2 SD of the bracketing standards used for correction, and was propagated in quadrature to the internal uncertainties (i.e., based on counting statistics) in order to assign a total uncertainty to each unknown; using this approach, the determined 2 SD external reproducibility of the measured $^{176}\text{Hf}/^{177}\text{Hf}$ from JMC-475 solutions varied for each set of unknowns from ± 0.000007 ($\pm 0.25 \epsilon\text{Hf}$) and ± 0.000011 ($\pm 0.39 \epsilon\text{Hf}$). Overall, 89 measurements of JMC-475 from three separate analytical sessions resulted in a $^{176}\text{Hf}/^{177}\text{Hf} = 0.282160 \pm 0.000009$ ($\pm 0.32 \epsilon\text{Hf}$), which agrees with the value of 0.282161 ± 0.000014 reported by Vervoort and Blichert-Toft (1999), and provides a reasonable measure of our reproducibility. Because this is the first contribution presenting Hf isotopic results from the MIT-IG laboratory, repeat runs of established zircon reference materials were also conducted in order to asses the accuracy of our results. Measurements conducted on dissolved single-crystals of FC1, 91500 and R33 gave $^{176}\text{Hf}/^{177}\text{Hf} = 0.282179 \pm 0.000012$ (2 SD), $^{176}\text{Hf}/^{177}\text{Hf} = 0.282305 \pm 0.000006$ (2 SD) and $^{176}\text{Hf}/^{177}\text{Hf} = 0.282751 \pm 0.000005$ (2 SD), respectively (Table DR3). These results are in

good agreement with their respective reference values (i.e., 0.282183 ± 0.000012 for FC1, Fisher et al., 2014; 0.282308 ± 0.000006 for 91500, Blichert-Toft, 2008; 0.282764 ± 0.000014 for R33, Fisher et al., 2014). Epsilon Hf (ϵ_{Hf}) values were calculated for each zircon using the values for the chondritic uniform reservoir (CHUR) presented in Bouvier et al. (2008). The 30 μl trace element aliquots were brought up in 1.0 ml of 3 % HNO_3 – 0.2 % HF solution, previously spiked with 2 ppb In. Trace element concentrations were measured by solution aspiration on an Agilent 7900 quadrupole-ICP-MS in the Center for Environmental Health Sciences at MIT, using a standardization scheme similar to that of Schoene et al. (2010). Calibration solutions were prepared gravimetrically from elemental standards to approximate the proportions expected in natural zircons, and mixed using the same In-spiked 3 % HNO_3 – 0.2 % HF solution used for our sample zircon aliquots as described above. The measured $^{176}\text{Lu}/^{177}\text{Hf}$ ratio for each crystal, calculated using the elemental Lu/Hf concentrations determined by quadrupole-ICP-MS and the natural Lu isotopic composition of Vervoort et al. (2004), was used to re-calculate the initial ϵ_{Hf} ($\epsilon_{\text{Hf(t)}}$) for each zircon at the crystallization age for each sample (Tables DR3 and DR4).

To assess the significance of the spread in $\epsilon_{\text{Hf(t)}}$ observed between the different samples, we constructed a curve for the Hf isotopic evolution of depleted Atlantic mantle (DAM) for the studied area. We compiled $^{176}\text{Hf}/^{177}\text{Hf}$ measurements for modern MORB collected between the Azores and the Charlie-Gibbs Fracture zone (Table DR5) and calculated a mean and 2σ variability (0.28327 ± 0.00013), which we assume to approximate the $^{176}\text{Hf}/^{177}\text{Hf}$ of the depleted mantle in this area. We projected the evolution of this reservoir back through time using a $^{176}\text{Lu}/^{177}\text{Hf}=0.03898$ calculated from the Bouvier et al. (2008) $^{176}\text{Lu}/^{177}\text{Hf}$ value for CHUR and the fractionation factor of $f=0.16$ from Vervoort and Blichert-Toft (1999) and the resulting $\epsilon_{\text{Hf,DAM}}$ curve is shown in Fig. 2. This figure includes previously published $\epsilon_{\text{Hf_i}}$ for gabbros that intrude exhumed mantle on the Iberia margin (Scharer et al., 2000) recalculated using the values for CHUR presented in Bouvier et al. (2008) and an average $^{176}\text{Lu}/^{177}\text{Hf}=0.0016$ for zircon (Faure and Mensing, 2005). All of the $\epsilon_{\text{Hf(t)}}$ values for magmas intruding exhumed mantle within the Newfoundland-Iberia rift are consistent with derivation from the depleted mantle in this area (Fig. 2).

Figure Captions

Figure DR1: A: Location of studied transects. B: Cross-sections of the two transects modified from Sutra et al. (2013) and Manatschal et al. (2001). The locations of all ODP drill sites that penetrated basement are shown. ODP site 1276 did not reach basement, but is also shown because it penetrated Cretaceous basaltic sills.

Figure DR2: Core recovery and lithology from ODP sites 1070 and 1277 modified from Shipboard Scientific Party (2004) and Jagoutz et al. (2007). The locations of $^{40}\text{Ar}/^{39}\text{Ar}$ and U-Pb dates (Tables 1 and DR1) from these two cores are also shown. Only analytical uncertainties are reported for samples dated as part of this study.

Figure DR3: Traditional U-Pb concordia diagrams for all dated samples showing $^{206}\text{Pb}/^{238}\text{U}$ and $^{207}\text{Pb}/^{235}\text{U}$ dates for each grain. Measurements that plot on the concordia curve represent agreement between the two isotopic systems.

Figure DR4: Rank order plot of Th-corrected $^{206}\text{Pb}/^{238}\text{U}$ zircon dates from ODP sites 1070 and 1277. Each bar represents a single zircon measurement and the horizontal black bar and gray rectangles represent the mean and 2σ uncertainty (internal), respectively. Duration uncertainty was calculated by adding the uncertainties of individual dates in quadrature.

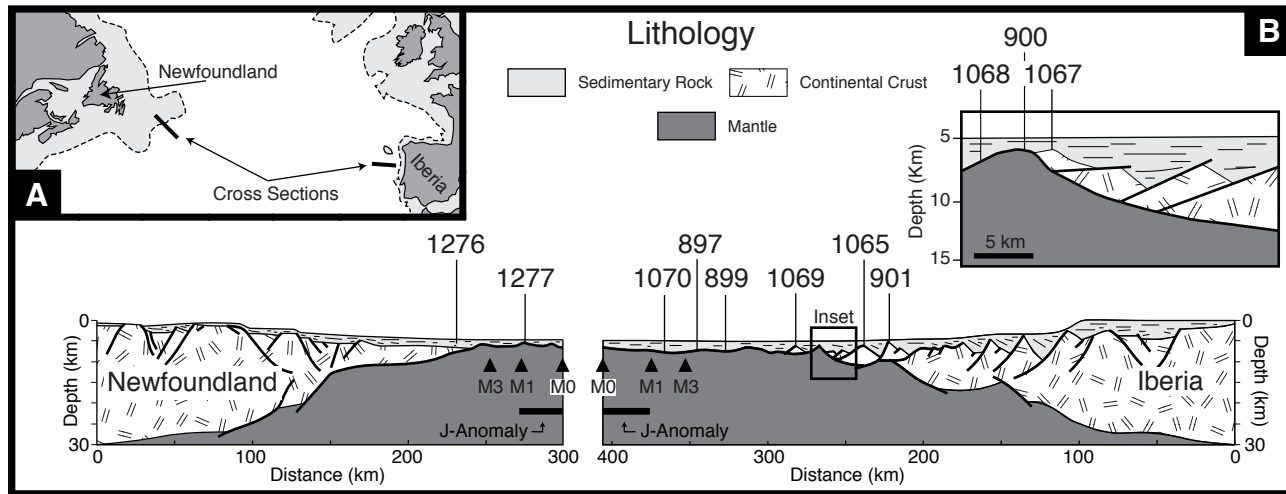
References

- Agranier, A., Blichert-Toft, J., Graham, D., Debaille, V., Schiano, P., and Albarede, F., 2005, The spectra of isotopic heterogeneities along the mid-Atlantic ridge: Earth and Planetary Science Letters, v. 238, p. 96-109, doi: 10.1016/j.epsl.2005.07.011.
- Andres, M., Blichert-Toft, J., and Schilling, J.G., 2004, Nature of the depleted upper mantle beneath the Atlantic: evidence from Hf isotopes in normal mid-ocean ridge basalts from 79°N to 55°S: Earth and Planetary Science Letters, v. 225, p. 89-103, doi: 10.1016/j.epsl.2004.05.041.
- Beard, J.S., Fullager, P.D., and Sinha, A.K., 2002, Gabbroic pegmatite intrusions, Iberia Abyssal Plain, ODP leg 173, site 1070: magmatism during a transition from non-volcanic rifting to seafloor spreading: Journal of Petrology, v. 43, p. 885-905, doi: 10.1093/petrology/43.5.885.
- Blichert-Toft, J., Agranier, A., Andres, M., Kingsley, R., Schilling, J.G., and Albarede, F., 2005, Geochemical segmentation of the Mid-Atlantic Ridge north of Iceland and ridge-hot spot interaction in the North Atlantic: Geochemistry, Geophysics, Geosystems, v. 6, Q01E19, doi: 10.1029/2004GC000788.
- Blichert-Toft, J., 2008, The Hf isotopic composition of zircon reference material 91500: Chemical Geology, v. 253, p. 252–257, doi: 10.1016/j.chemgeo.2008.05.014.
- Bouvier, A., Vervoort, J.D., and Patchett, P.J., 2008, The Lu-Hf and Sm-Nd isotopic composition of CHUR: constraints from unequilibrated chondrites and implications for the bulk composition of terrestrial planets: Earth and Planetary Science Letters, v. 273, p. 48-57, doi: 10.1016/j.epsl.2008.06.010.
- Bowring, J.F., McLean, N.M., and Bowring, S.A., 2011, Engineering cyber infrastructure for U-Pb geochronology: Tripoli and U-Pb_Redux: Geochemistry, Geophysics, and Geosystems, v. 12, doi: 10.1029/2010GC003479.
- Condon, D.J., Schoene, B., McLean, N.M., Bowring, S.A., and Parrish, R.R., 2015, Metrology and traceability of U-Pb isotopic dilution geochronology (EARTHTIME tracer calibration part I): Geochimica et Cosmochimica, v. 164, p 464-480, doi: 10.1016/j.gca.2015.05.026.
- Eddy, M.P., Bowring, S.A., Umhoefer, P.J., Miller, R.B., McLean, N.M., and Donaghay, E.E., 2016, High resolution temporal and stratigraphic record of Siletzia's accretion and triple junction migration from nonmarine sedimentary basins in central and western Washington: Geological Society of America Bulletin, doi: 10.1130/B31335.1.

- Faure, G., and Mensing, T.M., 2005, Isotopes: Principles and Applications: Hoboken, NJ, John Wiley and Sons, 897 p.
- Feraud, G., Beslier, M.O., and Cornen, G., 1996, $^{40}\text{Ar}/^{39}\text{Ar}$ dating of gabbros from the ocean/continent transition of the western Iberian margin: preliminary results, in, Whitmarsh, R.B., Sawyer, D.S., Klaus, A., and Masson, D.G., eds., Proceedings of the Ocean Drilling Program, Scientific Results, v. 149, p. 489-495, doi: 10.2973/odp.proc.sr.149.224.1996.
- Fisher, C. M., Vervoort, J. D., and DuFrane, S. A., 2014, Accurate Hf isotope determinations of complex zircons using the “laser ablation split stream” method: *Geochemistry Geophysics Geosystems*, v. 15, p. 121–139, doi: 10.1002/2013GC004962.
- Gale, A., Dalton, C.A., Langmuir, C.H., Su, Y. and Schilling, J.G., 2013, The mean composition of ocean ridge basalts: *Geochemistry, Geophysics, Geosystems*, v. 14, p. 489-518, doi: 10.1029/2012GC004334.
- Gardien, V., and Paquette, J.L., 2004, Ion microprobe and ID-TIMS U-Pb dating on zircon grains from Leg 173 amphibolites: evidence for Permian magmatism on the west Iberian margin: *Terra Nova*, v. 16, p. 226-231, doi: 10.1111/j.1365-3121.2004.00554.x.
- Jaffey, A.H., Flynn, K.F., Glendenin, L.E., Bentley, W.C., and Essling, A.M., 1971, Precision measurement of half-lives and specific activities of ^{235}U and ^{38}U : *Physical Review C*, v. 4, p. 1889-1906, doi: 10.1103/PhysRevC.4.1889.
- Goodge, J.W., and Vervoort, J.D., 2006, Origin of Mesoproterozoic A-type granites in Laurentia: Hf isotope evidence: *Earth and Planetary Science Letters*, v. 243, p. 711-731, doi: 10.1016/j.epsl.2006.01.040.
- Hart, S.R., and Blusztajn, 2006, Age and geochemistry of the mafic sills, ODP site 1276, Newfoundland margin: *Chemical Geology*, v. 235, p. 222-237, doi: 10.1016/j.chemgeo.2006.07.001.
- Jaffey, A.H., Flynn, K.F., Glendenin, L.E., Bentley, W.C., Essling, A.M., 1971, Precision measurement of half-lives and specific activities of ^{235}U and ^{38}U : *Physical Review C*, v. 4, p. 1889-1906, doi: 10.1103/PhysRevC.4.1889.
- Jagoutz, O., Muntener, O., Manatschal, G., Rubatto, D., Peron-Pinvidic, G., Turrin, B.D., and Villa, I.M., The rift-to-drift transition in the North Atlantic: A stuttering start of the MORB machine?: *Geology*, v. 35, p. 1087-1090, doi: 10.1130/G23613A.1.
- Kelley, K.A., Kingsley, R., and Schilling, J.G., 2013, Composition of plume-influenced mid-ocean ridge lavas and glasses from the Mid-Atlantic Ridge, East Pacific Rise, Galapagos Spreading Center, and Gulf of Aden: *Geochemistry, Geophysics, Geosystems*, v. 14, p. 223-242, doi: 10.1029/2012GC004415.
- Manatschal, G., Froitzheim, N., Rubenach, M., and Turrin, B.D., 2001, The role of detachment faulting in the formation of an ocean-continent transition : insights from the Iberia Abyssal Plain: *Geological Society Special Publications*, v. 187, p. 405-428, doi: 10.1144/GSL.SP.2001.187.01.20.
- Mattinson, J.M., 2005, Zircon U-Pb chemical abrasion (“CA-TIMS”) method: Combined annealing and multi-step partial dissolution analysis for improved precision and accuracy of zircon ages: *Chemical Geology*, v. 220, p. 47-66, doi: 10.1016/j.chemgeo.2005.03.011.

- McLean, N.M., Bowring, J.F., and Bowring, S.A., 2011, An algorithm for U-Pb isotope dilution data reduction and uncertainty propagation: *Geochemistry, Geophysics, Geosystems*, v. 12, Q0AA19, doi: 10.1029/2010GC003478.
- McLean, N.M., Condon, D.J., Condon, B., and Bowring, S.A., 2015, Evaluating uncertainties in the calibration of isotopic reference materials and multi-element isotopic tracers (EARTHTIME tracer calibration II): *Geochimica et Cosmochimica*, v. 164, p. 481-501, doi: 10.1016/j.gca.2015.02.040.
- Muntener, O., and Manatschal, G., 2006, High degrees of melt extraction recorded by spinel harzburgite of the Newfoundland margin: the role of inheritance and consequences for the evolution of the southern North Atlantic: *Earth and Planetary Science Letters*, v. 252, p. 437-452, doi: 10.1016/j.epsl.2006.10.009.
- Peron-Pinvidic, G., and Manatschal, G., 2009, The final rifting evolution at deep magma-poor passive margins from Iberia-Newfoundland: a new point of view: *International Journal of Earth Science*, v. 98, p. 1581-1597, doi: 10.1007/s00531-008-0337-9 .
- Scharer, U., Girardeau, J., Cornen, G., and Boillot, G., 2000, 138-121 Ma asthenospheric magmatism prior to continental break-up in the North Atlantic and geodynamic implications: *Earth and Planetary Science Letters*, v. 181, p. 555-572, doi: 10.1016/S0012-821X(00)00220-X.
- Scharer, U., 1984, The effect of initial ^{230}Th disequilibrium on young U-Pb ages: the Makalu case, Himalaya: *Earth and Planetary Science Letters*, v. 67, p. 191-204, doi: 10.1016/0012-821X(84)90114-6.
- Schoene, B., Latkoczy, C., Schaltegger, U., and Gunther, D., 2010, A new method integrating high-precision U-Pb geochronology with zircon trace element analysis (U-Pb TIMS-TEA): *Geochimica et Cosmochimica Acta*, v. 74, p. 7144-7159, doi: 10.1016/j.gca.2010.09.016.
- Shipboard Scientific Party, 1994, Site 897, *in* Sawyer, D.S., Whitmarsh, R.B., Klaus, A., et al. (eds.): *Proceedings of the Ocean Drilling Program, Initial Reports*, v. 149, p. 41-113, doi: 10.2973/odp.proc.ir.149.104.1994.
- Shipboard Scientific Party, 1994, Site 899, *in* Sawyer, D.S., Whitmarsh, R.B., Klaus, A., et al. (eds.): *Proceedings of the Ocean Drilling Program, Initial Reports*, v. 149, p. 147-209, doi: 10.2973/odp.proc.ir.149.106.1994.
- Shipboard Scientific Party, 2004, Site 1277, *in* Tucholke, B.E., Sibuet, J.-C., Klaus, A., et al., (eds.): *Proceedings of the Ocean Drilling Program, Initial Reports*, v. 210, p. 1-39, doi: 10.2973/odp.proc.ir.210.104.2004.
- Soderlund, U., Patchett, P.J., Vervoort, J.D., and Isachsen, C.E., 2004, The ^{176}Lu decay constant determined by Lu-Hf and U-Pb isotope systematics of Precambrian mafic intrusions: *Earth and Planetary Science Letters*, v. 219, p. 311-324, doi: 10.1016/S0012-821X(04)00012-3.
- Vervoort, J.D., and Blichert-Toft, J., 1999, Evolution of the depleted mantle: Hf isotope evidence from juvenile rocks through time: *Geochimica et Cosmochimica Acta*, v. 63, p. 533-556, doi: 10.1016/S0016-7037(98)00274-9.
- Vervoort, J.D., Patchett, P.J., Soderlund, U., and Baker, M., 2004, Isotopic composition of Yb and the determination of Lu concentrations and Lu/Hf ratios by isotope dilution using MC-ICPMs: *Geochemistry, Geophysics, Geosystems*, v. 5, Q11002, doi: 10.1029/2004GC000721.

FIGURE DR1



ODP Leg 210 Site 1277

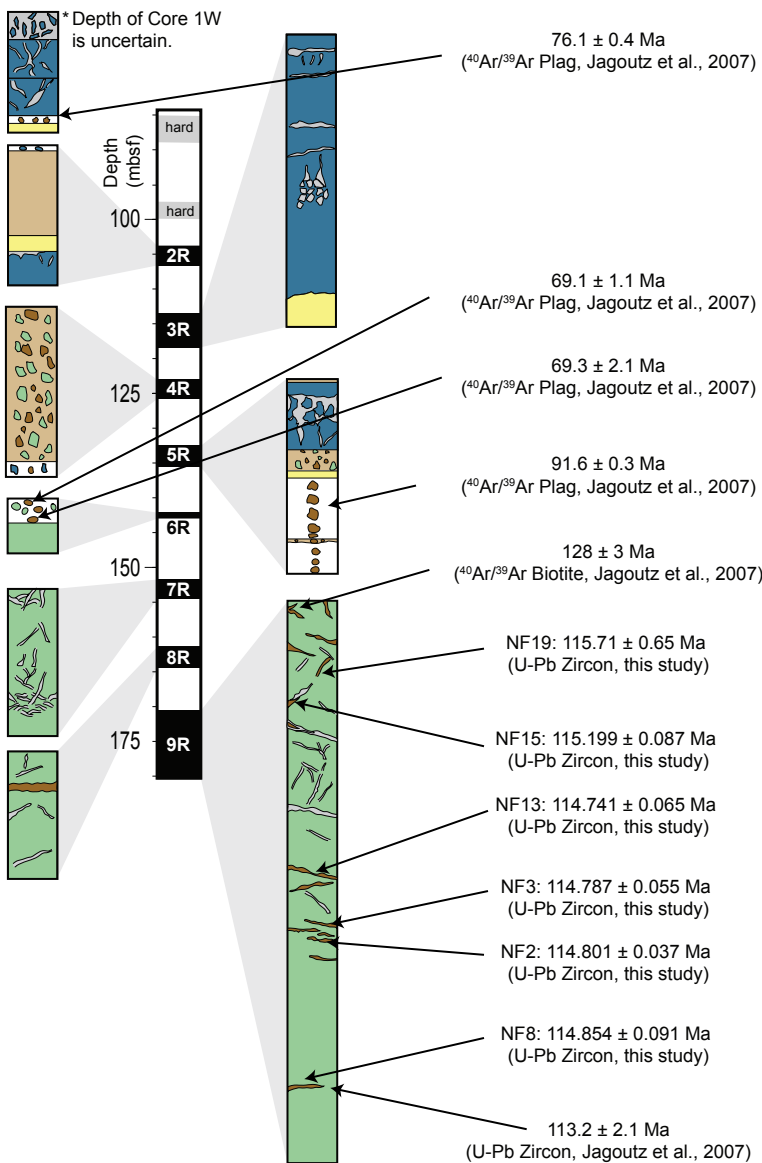
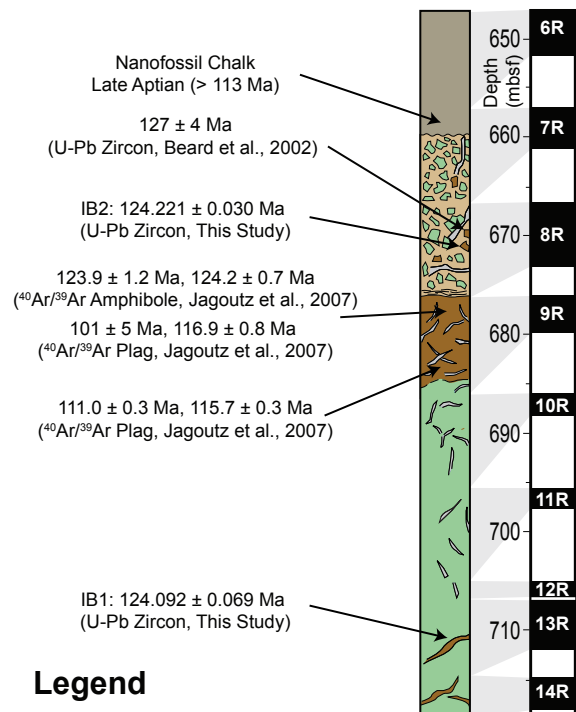


FIGURE DR2

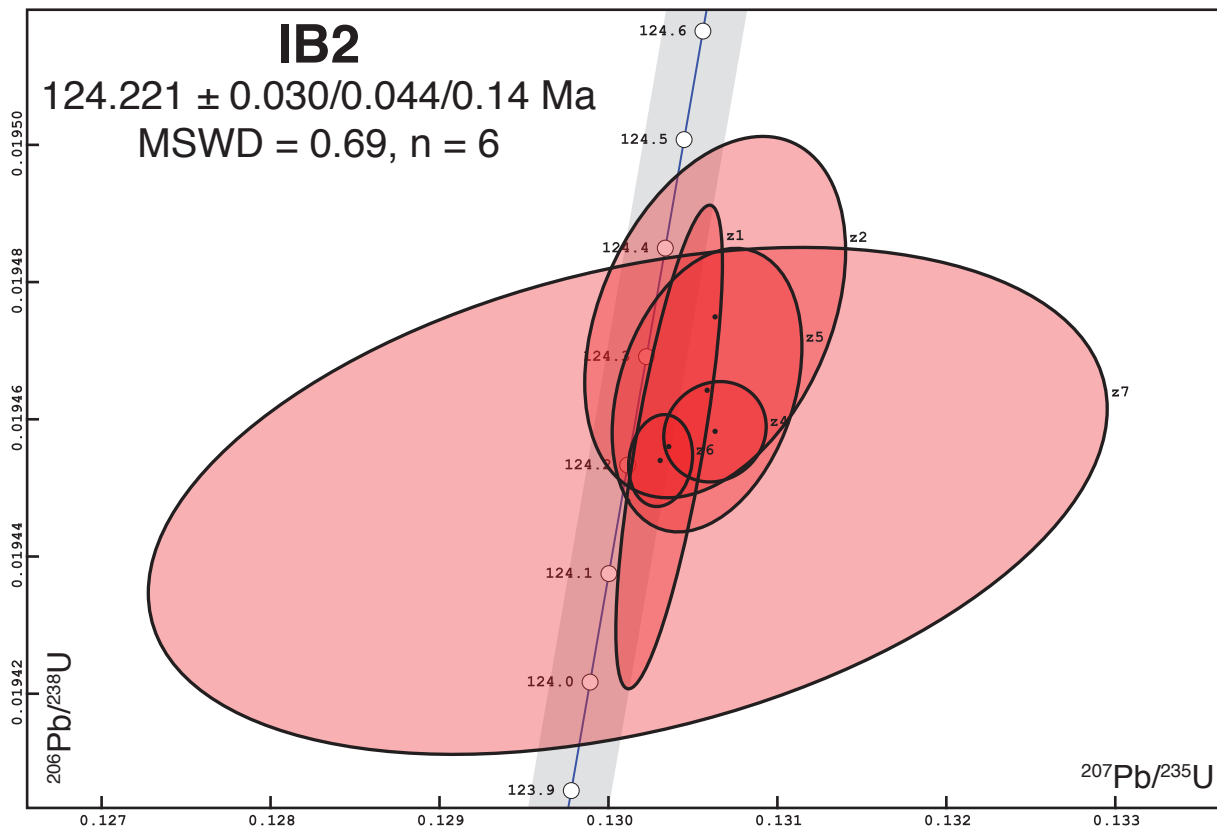
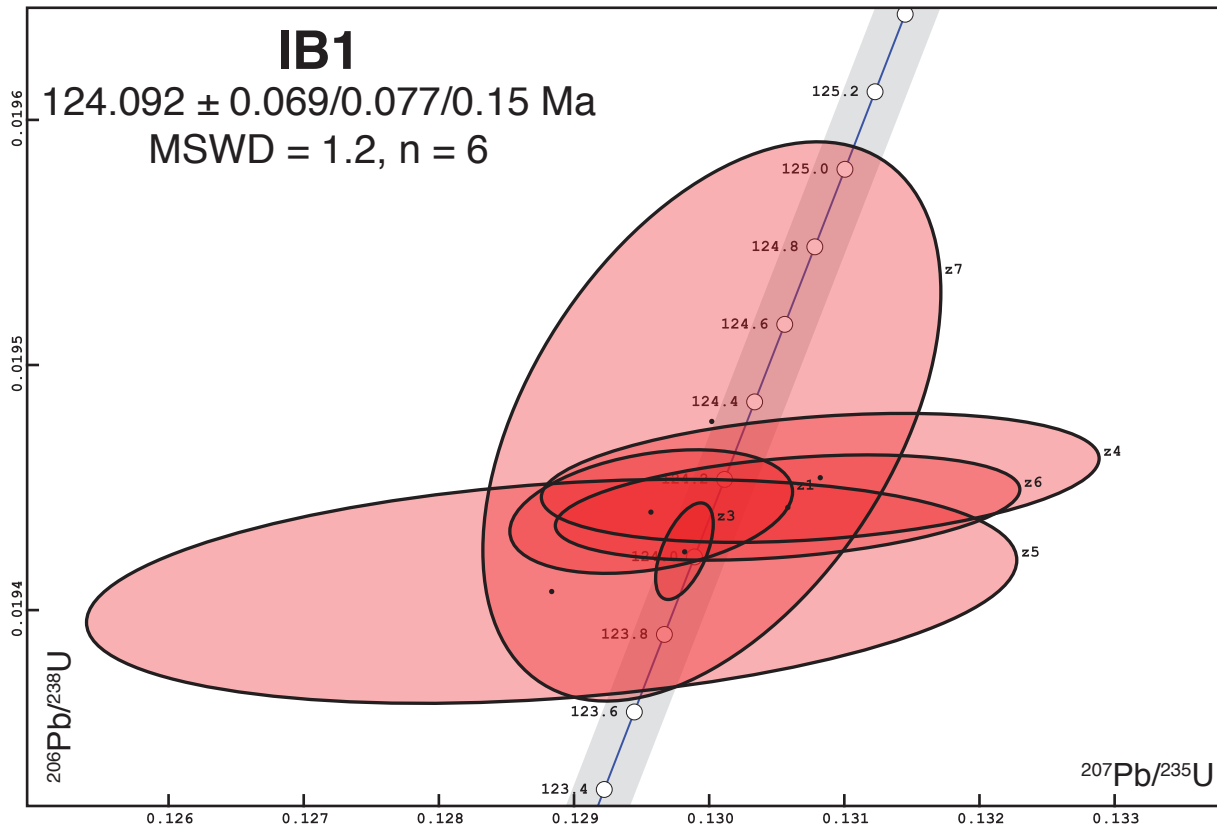
ODP Leg 173 Site 1070

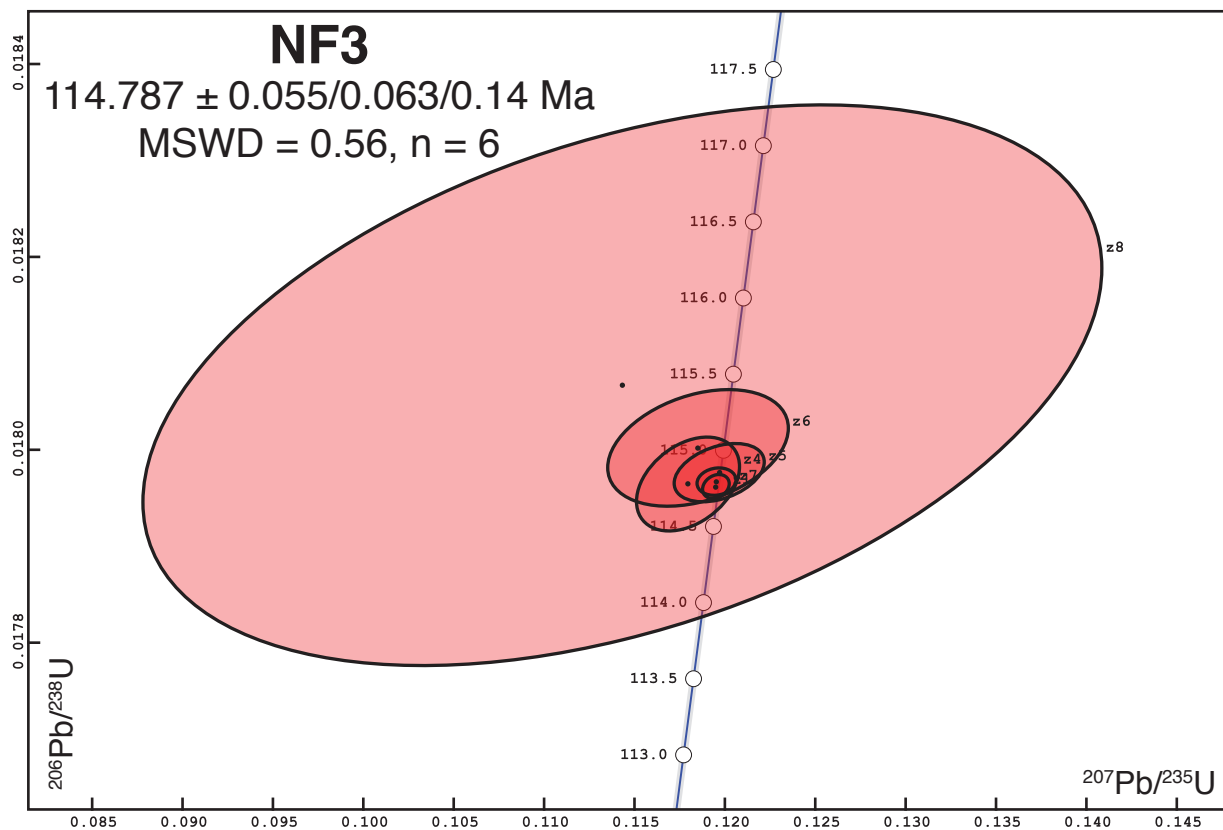
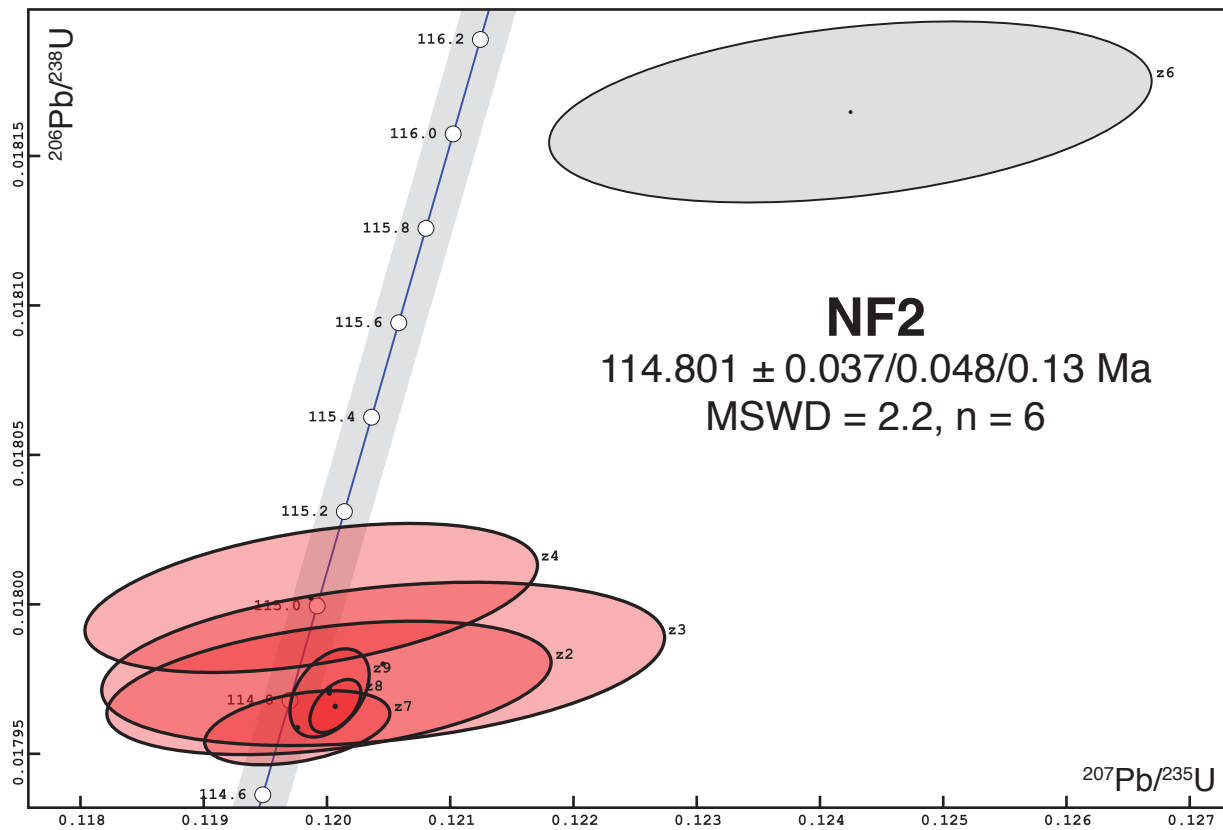


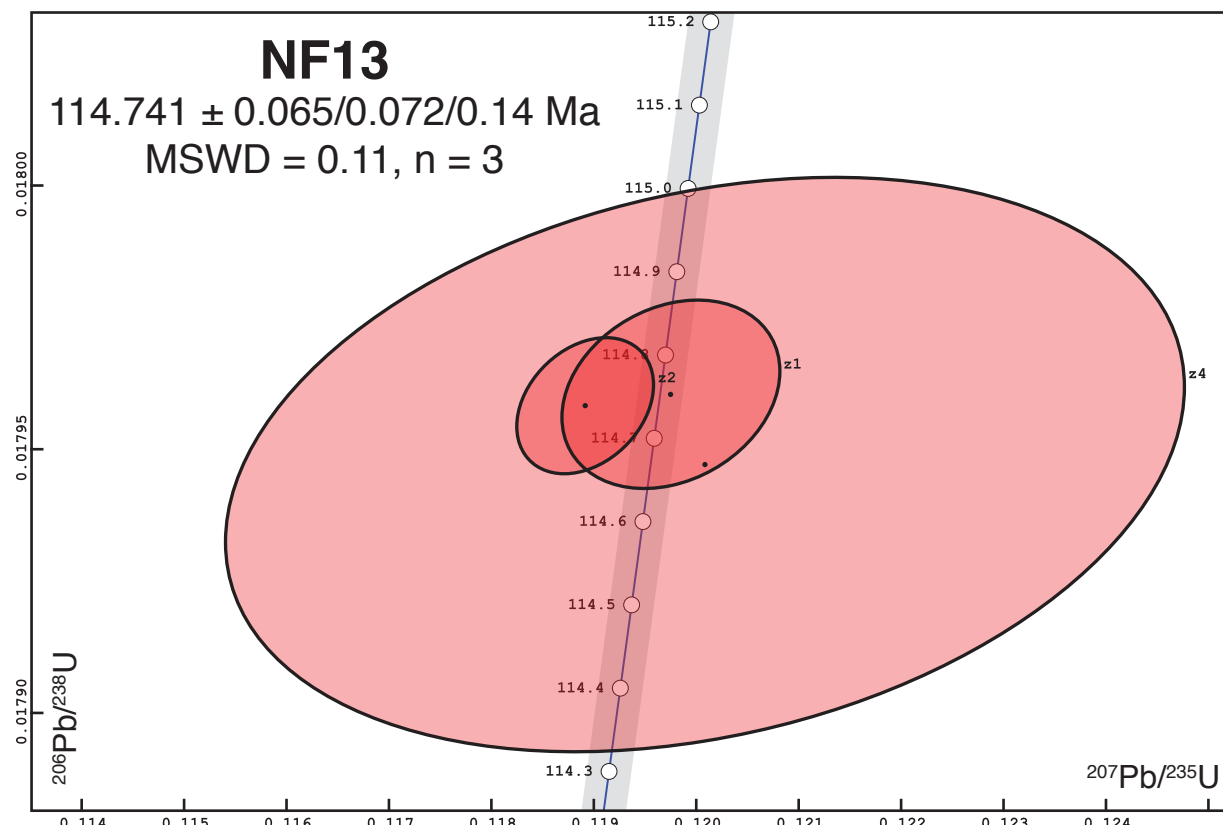
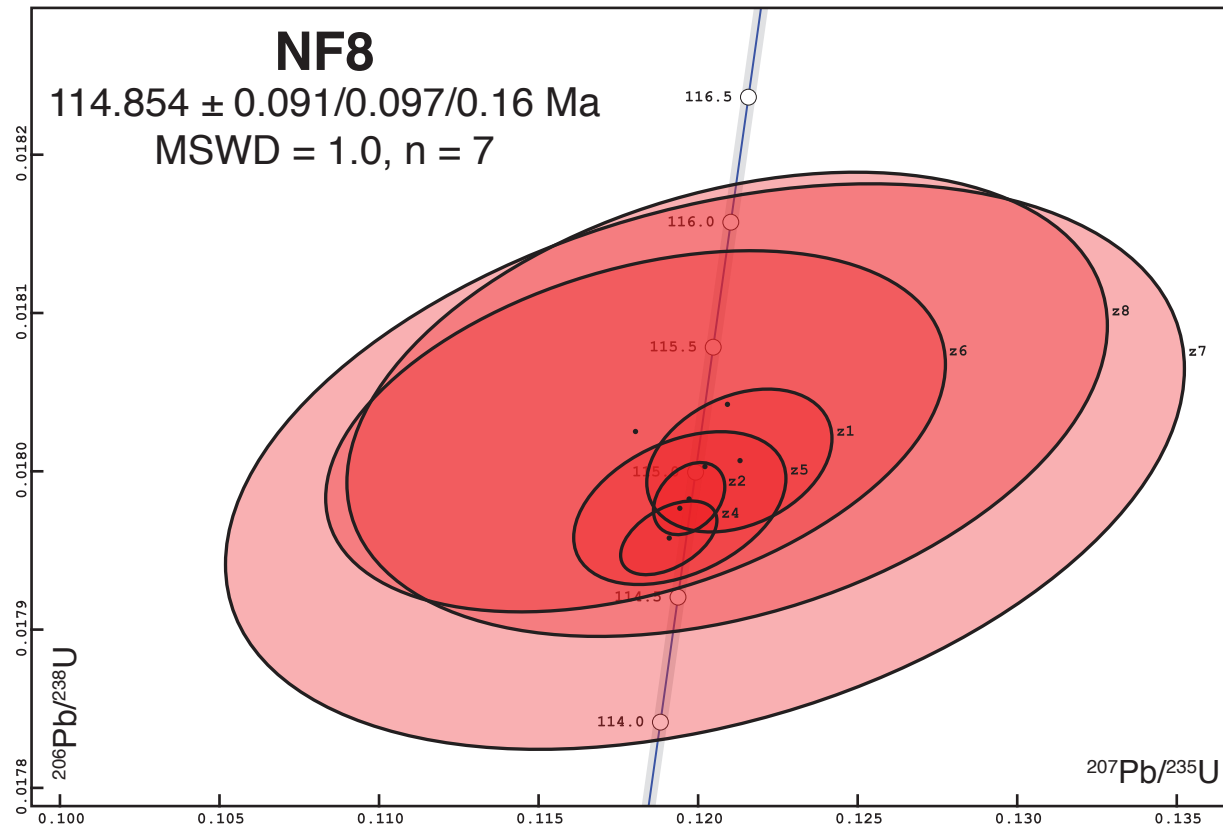
Legend

Clay
Basalt
Sandstone
Tectonosedimentary Breccia (Lithology of Large Clasts is Shown)
Gabbro
Serpentinized Peridotite
Magmatic Veins (Brown) Calcite/Serpentinite Veins (Gray)

FIGURE DR3







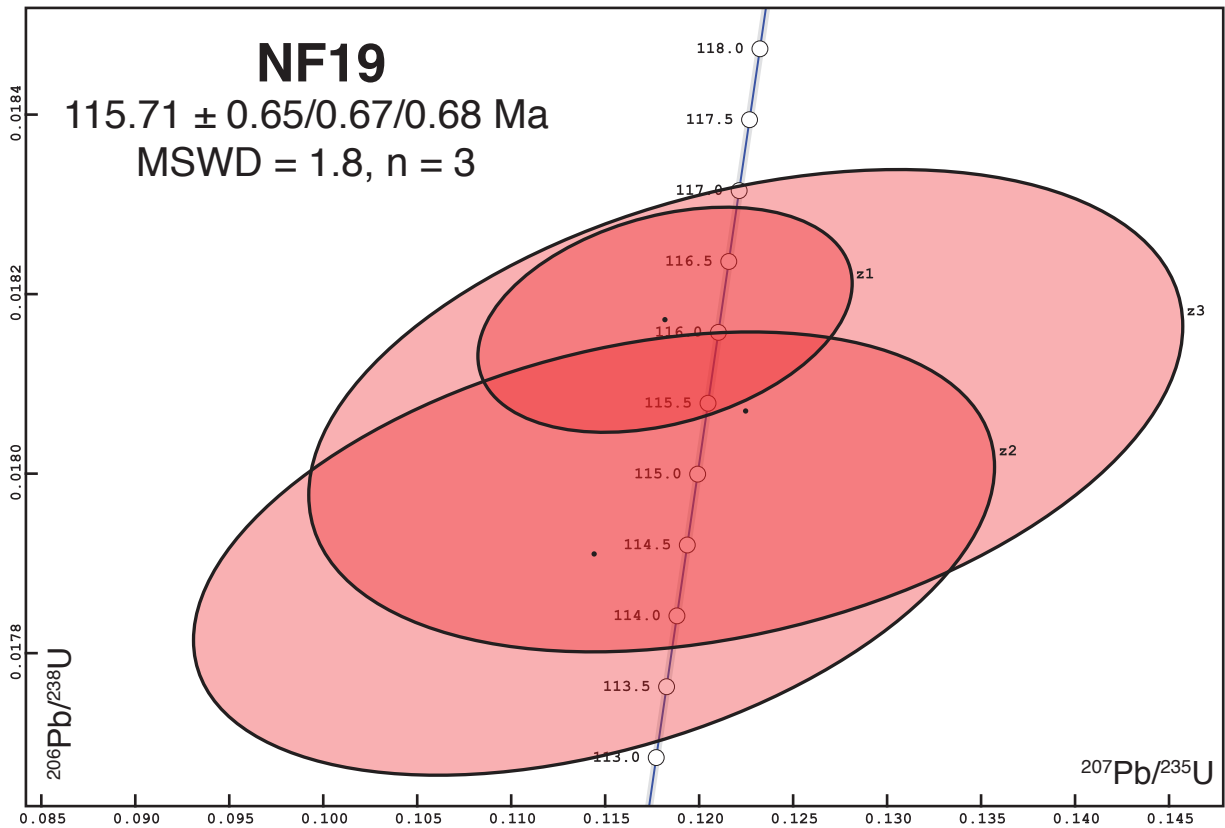
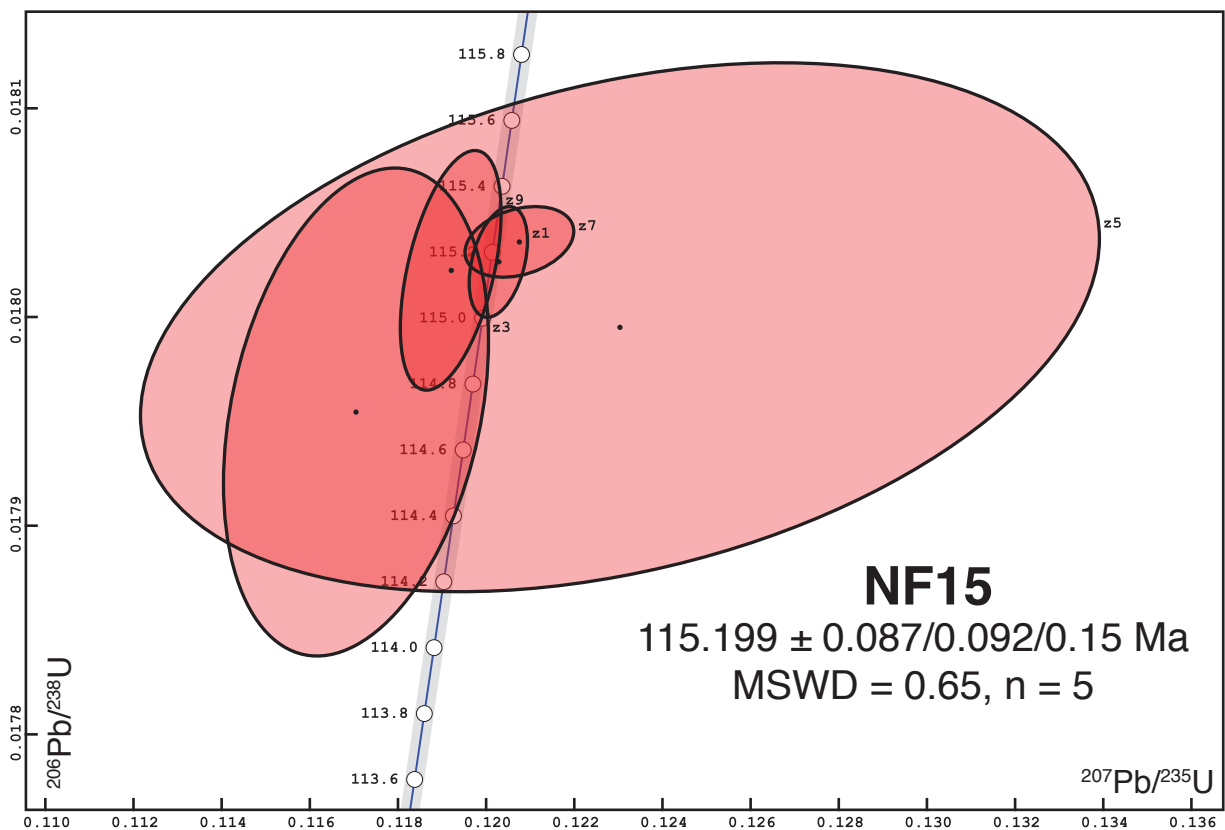


Figure DR4

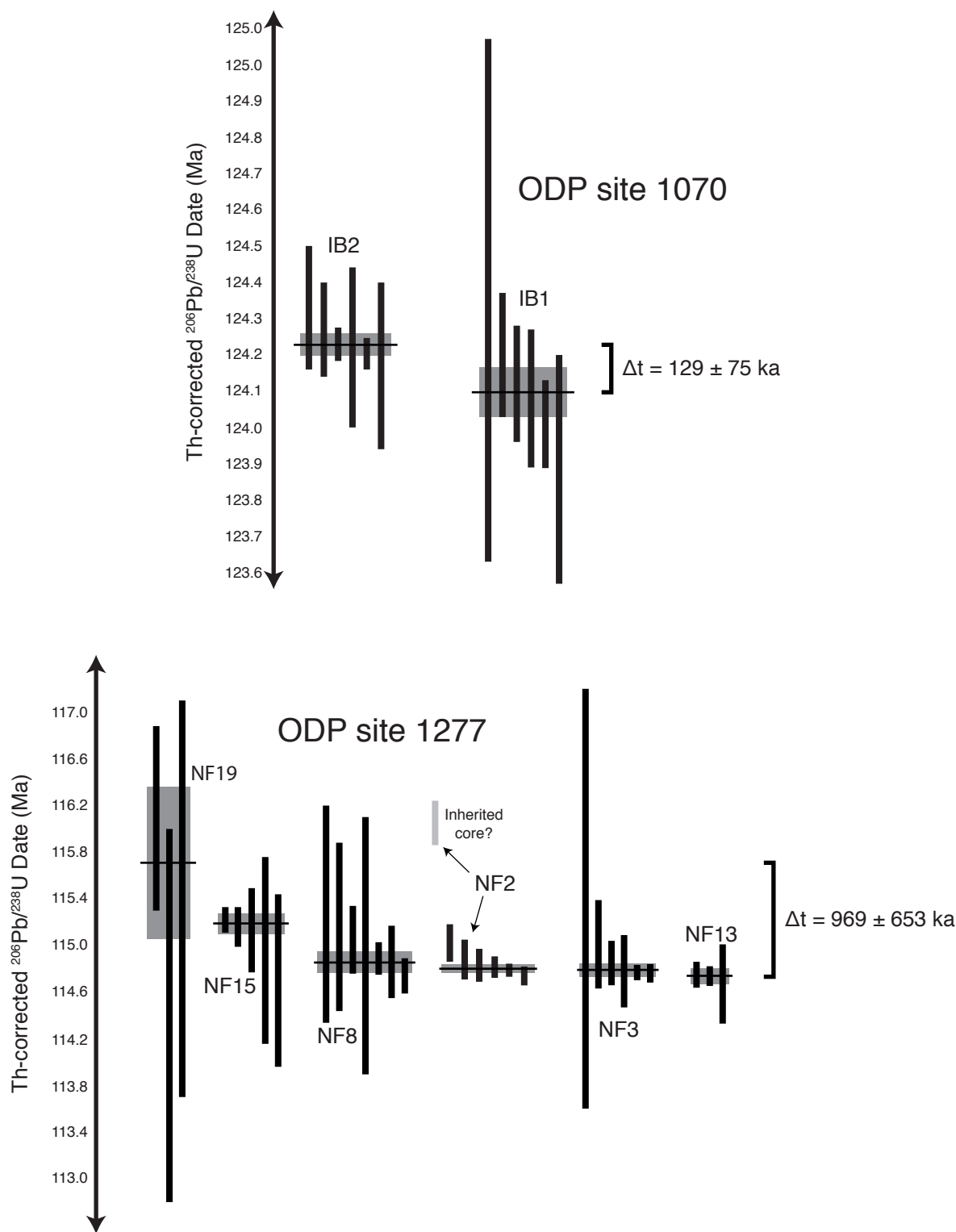


TABLE DR1: PREVIOUS GEO- AND THERMOCHRONOLOGY

ODP Site	Lithology	Mineral	$^{40}\text{Ar}/^{39}\text{Ar}$ Date (Ma)	2σ (Ma)	U-Pb Date (Ma)	2σ (Ma)	Reference
1067	Amphibolite	Amphibole	160.5	0.8	-	-	Jagoutz et al. (2007)
1067	Amphibolite	Amphibole	152.6	0.9	-	-	Jagoutz et al. (2007)
1067	Amphibolite	Plagioclase	141.8	0.4	-	-	Jagoutz et al. (2007)
1067	Amphibolite	Amphibole	164.6	0.5	-	-	Jagoutz et al. (2007)
1067	Amphibolite	Amphibole	167.3	0.9	-	-	Jagoutz et al. (2007)
1067	Amphibolite	Zircon	-	-	246.0	5.0	Gardien and Paquette (2004)
900	Gabbro	Plagioclase	136.4	0.6	-	-	Feraud et al. (1996)
1068	Gabbro	Plagioclase	133.1	0.3	-	-	Jagoutz et al. (2007)
1068	Gabbro	Amphibole	131.7	1.1	-	-	Jagoutz et al. (2007)
1068	Gabbro	Amphibole	140.0	2.0	-	-	Jagoutz et al. (2007)
1069	Schist	Muscovite	361.5	0.5	-	-	Jagoutz et al. (2007)
1070	Gabbro	Plagioclase	115.7	0.3	-	-	Jagoutz et al. (2007)
1070	Gabbro	Plagioclase	111.0	0.3	-	-	Jagoutz et al. (2007)
1070	Gabbro	Plagioclase	116.9	0.8	-	-	Jagoutz et al. (2007)
1070	Gabbro	Amphibole	123.9	1.2	-	-	Jagoutz et al. (2007)
1070	Gabbroic Clast	Zircon	-	-	127.0	4.0	Beard et al. (2002)
1277	Gabbro	Zircon	-	-	113.2	2.1	Jagoutz et al. (2007)
1277	Gabbro	Biotite	128.0	3.0	-	-	Jagoutz et al. (2007)
1277	Gabbroic Clast	Plagioclase	69.3	2.1	-	-	Jagoutz et al. (2007)
1277	Gabbroic Clast	Plagioclase	69.1	1.1	-	-	Jagoutz et al. (2007)
1277	Gabbroic Clast	Plagioclase	91.6	0.3	-	-	Jagoutz et al. (2007)
1277	Gabbroic Clast	Plagioclase	76.1	0.4	-	-	Jagoutz et al. (2007)
1276	Basaltic Sill	Whole Rock	104.7	1.7	-	-	Hart and Blujstein (2006)
1276	Basaltic Sill	Whole Rock	105.9	1.8	-	-	Hart and Blujstein (2006)
1276	Basaltic Sill	Whole Rock	99.7	1.8	-	-	Hart and Blujstein (2006)
1276	Basaltic Sill	Whole Rock	95.9	2.0	-	-	Hart and Blujstein (2006)

TABLE DR2: CA-ID-TIMS U-Pb ZIRCON GEOCHRONOLOGY RESULTS

Frac.	Dates		Composition						Isotopic Ratios										
	$^{206}\text{Pb}/^{238}\text{U}^*$	2 σ abs.	$^{207}\text{Pb}/^{235}\text{U}^\dagger$	2 σ abs.	$^{207}\text{Pb}/^{206}\text{Pb}^{\ddagger,\dagger}$	2 σ abs.	% Disc. §	Corr. Coef.	Th/U [#]	Pb _{c,*} (pg)	Pb*/Pb _{c,††}	$^{206}\text{Pb}/^{204}\text{Pb}^{\$§}$	$^{206}\text{Pb}/^{206}\text{Pb}^{\#§}$	$^{206}\text{Pb}/^{238}\text{U}^{*\#\#}$	2 σ %	$^{207}\text{Pb}/^{235}\text{U}^{\#\#}$	2 σ %	$^{207}\text{Pb}/^{206}\text{Pb}^{\#\#}$	2 σ %
<u>IB1 (13R-4 36-42)</u>																			
z1	124.12	0.16	123.71	0.94	116	18	-5.55	0.320	0.79	0.31	31	1734	0.252	0.019440	0.13	0.1296	0.81	0.048362	0.77
z3	124.01	0.12	123.93	0.19	122.4	3.2	0.03	0.564	0.76	0.36	184	10273	0.243	0.019424	0.10	0.12982	0.16	0.048494	0.13
z4	124.20	0.17	124.8	1.9	137	36	10.40	0.302	0.67	1.48	14	793	0.214	0.019454	0.14	0.1308	1.6	0.048795	1.5
z5	123.91	0.29	123.0	3.1	106	62	-14.75	0.279	0.96	0.45	10	530	0.306	0.019407	0.24	0.1288	2.7	0.048168	2.6
z6	124.13	0.14	124.6	1.5	134	30	8.48	0.344	0.86	0.59	18	973	0.274	0.019442	0.11	0.1306	1.3	0.048735	1.3
z7	124.35	0.72	124.1	1.5	120	27	-2.57	0.462	0.88	0.42	24	1298	0.281	0.019477	0.59	0.1300	1.3	0.048438	1.2
<u>IB2 (8R-4 11-17)</u>																			
z1	124.22	0.22	124.42	0.28	128.3	3.7	4.43	0.761	0.79	0.45	175	9662	0.252	0.019456	0.18	0.13036	0.24	0.048617	0.15
z2	124.33	0.17	124.67	0.69	131	13	6.23	0.366	0.79	0.38	47	2607	0.252	0.019475	0.14	0.13063	0.59	0.048671	0.56
z4	124.230	0.046	124.66	0.27	133.0	5.4	7.77	0.101	0.62	0.36	115	6633	0.198	0.019458	0.038	0.13063	0.23	0.048713	0.23
z5	124.27	0.13	124.62	0.50	131.4	9.7	6.58	0.305	0.78	0.30	58	3209	0.249	0.019464	0.11	0.13058	0.43	0.048680	0.41
z6	124.203	0.043	124.37	0.17	127.7	3.4	3.99	0.120	0.69	0.40	176	10006	0.218	0.019454	0.035	0.13031	0.15	0.048603	0.14
z7	124.17	0.23	124.2	2.5	125	50	1.90	0.364	0.68	0.58	10	614	0.216	0.019448	0.19	0.1301	2.2	0.048545	2.1
<u>NF2 (9R-5 50-56)</u>																			
z2	114.83	0.14	115.1	1.6	120	34	6.20	0.382	0.58	0.43	15	905	0.186	0.017972	0.12	0.1200	1.5	0.048455	1.5
z3	114.88	0.17	115.5	2.1	128	44	11.73	0.323	0.33	0.55	11	712	0.105	0.017980	0.15	0.1205	1.9	0.048611	1.9
z4	115.02	0.16	115.0	1.7	114	35	0.62	0.438	0.42	0.29	14	895	0.132	0.018002	0.14	0.1199	1.5	0.048316	1.5
z6	116.05	0.19	118.9	2.2	177	45	35.09	0.340	0.37	0.44	10	650	0.118	0.018165	0.17	0.1242	2.0	0.049631	1.9
z7	114.741	0.079	114.85	0.68	117	14	3.75	0.387	0.42	0.59	36	2189	0.132	0.017959	0.069	0.11976	0.63	0.048387	0.60
z8	114.788	0.056	115.13	0.19	122.3	3.6	7.82	0.507	0.15	0.29	149	9813	0.046	0.017966	0.049	0.12007	0.17	0.048492	0.15
z9	114.815	0.093	115.09	0.29	120.8	5.8	6.59	0.406	0.31	1.01	80	5064	0.098	0.017970	0.082	0.12002	0.27	0.048462	0.24
<u>NF3 (9R-5 26-33)</u>																			
z1	114.761	0.079	114.62	0.67	112	14	-0.89	0.232	0.43	0.37	35	2152	0.136	0.017962	0.069	0.11950	0.62	0.048275	0.60
z4	114.78	0.31	113.2	2.6	81	55	-39.11	0.372	0.63	0.46	10	595	0.200	0.017964	0.27	0.1180	2.4	0.047646	2.3
z5	114.85	0.19	114.8	2.3	113	48	0.46	0.365	0.57	0.51	11	652	0.182	0.017976	0.17	0.1197	2.1	0.048311	2.0
z6	115.01	0.38	113.7	4.5	87	98	-29.61	0.339	0.52	0.32	5	320	0.167	0.018002	0.34	0.1185	4.2	0.047770	4.1
z7	114.793	0.090	114.65	0.98	112	21	-1.01	0.128	0.58	0.35	25	1489	0.184	0.017967	0.079	0.1195	0.90	0.048276	0.89
z8	115.4	1.8	110	24	-8	540	2078.78	0.418	0.40	0.28	1	81	0.127	0.018067	1.6	0.114	23	0.045917	23
<u>NF8 (9R-7 45-50)</u>																			
z1	115.05	0.29	116.2	2.6	141	55	19.43	0.309	0.52	0.32	9	565	0.166	0.018007	0.25	0.1213	2.4	0.048876	2.3
z2	114.89	0.14	114.8	1.0	113	21	0.26	0.323	0.47	0.30	24	1476	0.150	0.017983	0.13	0.1197	0.93	0.048306	0.90
z4	114.74	0.15	114.2	1.4	104	29	-8.42	0.472	0.48	0.36	19	1144	0.153	0.017958	0.13	0.1191	1.3	0.048115	1.2
z5	114.86	0.31	114.6	3.0	108	64	-4.21	0.387	0.49	0.42	8	489	0.157	0.017977	0.27	0.1194	2.8	0.048204	2.7
z6	115.16	0.72	113.3	8.8	74	190	-51.26	0.371	0.48	0.35	3	180	0.153	0.018025	0.63	0.1180	8.2	0.047516	8.0
z7	115.0	1.1	115	14	120	290	5.96	0.347	0.46	1.49	2	119	0.147	0.018003	0.99	0.120	12	0.048452	12
z8	115.27	0.93	116	11	129	230	11.83	0.339	0.48	0.98	2	148	0.153	0.018042	0.81	0.121	9.9	0.048626	9.6
<u>NF13 (9R-4 56-64)</u>																			
z1	114.75	0.11	114.85	0.96	117	20	3.56	0.246	0.24	0.36	23	1500	0.076	0.017960	0.099	0.1198	0.89	0.048380	0.87
z2	114.739	0.082	114.09	0.61	101	13	-11.78	0.305	0.31	0.59	38	2424	0.099	0.017958	0.072	0.11892	0.56	0.048047	0.54
z4	114.67	0.34	115.1	4.2	125	90	9.83	0.271	0.38	0.58	6	389	0.122	0.017947	0.30	0.1201	3.9	0.048550	3.8
<u>NF15 (9R-2 11-17)</u>																			
z1	115.17	0.17	115.32	0.60	118	12	4.38	0.380	0.51	0.38	69	4136	0.163	0.018026	0.15	0.12028	0.55	0.048414	0.51
z3	114.71	0.74	112.4	2.7	63	59	-75.60	0.294	0.64	1.07	10	571	0.205	0.017954	0.65	0.1170	2.6	0.047303	2.5
z5	114.97	0.80	117.8	9.8	176	200	35.32	0.335	0.46	1.14	2	156	0.147	0.017995	0.70	0.123	8.8	0.049611	8.6
z7	115.23	0.11	115.8	1.1	127	23	10.30	0.297	0.59	0.82	21	1238	0.188	0.018036	0.094	0.1208	1.0	0.048580	1.0

z9	115.14	0.36	114.3	1.0	98	20	-15.83	0.481	0.88	0.69	43	2354	0.280	0.018022	0.32	0.1192	0.96	0.047990	0.85
<u>NF19 (9R-1 146-148)</u>																			
z1	116.09	0.79	113.4	9.0	58	200	-94.21	0.323	0.57	0.33	3	172	0.180	0.018171	0.69	0.118	8.4	0.047192	8.2
z2	114.4	1.6	110	19	15	440	-588.85	0.392	0.51	0.35	1	96	0.164	0.017911	1.4	0.114	19	0.046348	18
z3	115.4	1.7	117	21	155	430	26.72	0.351	0.32	0.37	1	84	0.101	0.018070	1.5	0.122	19	0.049182	19

Corrected for initial Th/U disequilibrium using radiogenic ^{208}Pb and Th/U_{Magma} = 3.2 ± 1 (2 σ) from the Gale et al. (2013) average MORB composition.

[†] Isotopic dates calculated using the decay constants $\lambda_{238} = 1.55125\text{E-}10$ and $\lambda_{235} = 9.8485\text{E-}10$ (Jaffey et al. 1971).

[§] % discordance = 100 - (100 * ($^{206}\text{Pb}/^{238}\text{U}$ date) / ($^{207}\text{Pb}/^{206}\text{Pb}$ date))

[#] Th contents calculated from radiogenic ^{208}Pb and the $^{207}\text{Pb}/^{206}\text{Pb}$ date of the sample, assuming concordance between U-Th and Pb systems.

^{..} Total mass of common Pb.

^{††} Ratio of radiogenic Pb (including ^{208}Pb) to common Pb.

^{§§} Measured ratio corrected for fractionation and spike contribution only.

^{##} Measured ratios corrected for fractionation, tracer and blank.

TABLE DR3: Hf ISOTOPIC RESULTS

Frac.	$^{176}\text{Lu}/^{177}\text{Hf}^*$	$\pm 2\sigma_{\text{int}}^{\text{T}}$	$\pm 2\sigma_{\text{tot}}^{\text{s}}$	$^{176}\text{Lu}/^{177}\text{Hf}^{\#}$	Age (Ma)	$^{176}\text{Hf}/^{177}\text{Hf}_{(0)}^{**}$	$\pm 2\sigma^{\text{TT}}$	$\epsilon\text{Hf}_{(0)}$	$\pm 2\sigma$	Total Hf (V)
<u>IB1 (13R-4 36-42)</u>										
z1	0.283078	0.000002	0.000008	0.0008	124.092	0.283076	0.000008	13.04	0.27	75.8
z3	0.283066	0.000002	0.000010	0.0005	124.092	0.283064	0.000010	12.64	0.35	76.3
z4	0.283068	0.000002	0.000010	0.0005	124.092	0.283066	0.000010	12.71	0.35	96.6
z5	0.283070	0.000006	0.000009	0.0008	124.092	0.283069	0.000009	12.79	0.33	10.7
z6	0.283070	0.000002	0.000010	0.0008	124.092	0.283068	0.000010	12.76	0.35	56.1
z7	0.283073	0.000002	0.000008	0.0009	124.092	0.283071	0.000008	12.88	0.28	62.7
<u>IB2 (8R-4 11-17)</u>										
z1	0.283074	0.000002	0.000010	0.0024	124.221	0.283068	0.000010	12.78	0.34	167.4
z2	0.283071	0.000002	0.000010	0.0021	124.221	0.283066	0.000010	12.70	0.35	78.0
z4	0.283077	0.000002	0.000009	0.0019	124.221	0.283072	0.000009	12.92	0.31	190.1
z5	0.283061	0.000002	0.000010	0.0012	124.221	0.283058	0.000010	12.43	0.34	132.1
z6	0.283060	0.000002	0.000010	0.0020	124.221	0.283055	0.000010	12.33	0.35	125.3
z7	0.283079	0.000007	0.000010	0.0014	124.221	0.283075	0.000010	13.03	0.36	8.3
<u>NF2 (9R-5 50-56)</u>										
z1	0.283206	0.000011	0.000014	0.0035	114.801	0.283199	0.000014	17.18	0.51	4.7
z2	0.283194	0.000006	0.000011	0.0041	114.801	0.283185	0.000011	16.70	0.39	11.4
z3	0.283190	0.000007	0.000012	0.0039	114.801	0.283182	0.000012	16.59	0.41	11.7
z4	0.283197	0.000007	0.000010	0.0042	114.801	0.283188	0.000010	16.82	0.36	7.5
z5	0.283198	0.000006	0.000010	0.0047	114.801	0.283188	0.000010	16.82	0.34	12.1
z6	0.283185	0.000005	0.000011	0.0029	114.801	0.283179	0.000011	16.49	0.38	12.7
z7	0.283199	0.000005	0.000010	0.0044	114.801	0.283189	0.000010	16.85	0.37	16.5
z8	0.283197	0.000003	0.000010	0.0056	114.801	0.283185	0.000010	16.69	0.36	29.7
z9	0.283189	0.000003	0.000012	0.0039	114.801	0.283181	0.000012	16.55	0.45	84.1
<u>NF3 (9R-5 26-33)</u>										
z1	0.283194	0.000005	0.000011	0.0030	114.787	0.283187	0.000011	16.78	0.38	12.7
z4	0.283191	0.000007	0.000012	0.0025	114.787	0.283185	0.000012	16.71	0.42	8.0
z5	0.283177	0.000008	0.000012	0.0034	114.787	0.283169	0.000012	16.14	0.44	7.4
z6	0.283199	0.000008	0.000011	0.0030	114.787	0.283192	0.000011	16.95	0.38	6.1
z7	0.283197	0.000004	0.000008	0.0037	114.787	0.283189	0.000008	16.84	0.30	20.9
z8	0.283180	0.000011	0.000016	0.0006	114.787	0.283178	0.000016	16.46	0.58	4.1
<u>NF8 (9R-7 45-50)</u>										
z1	0.283185	0.000004	0.000010	0.0013	114.854	0.283182	0.000010	16.59	0.36	34.3
z2	0.283196	0.000004	0.000010	0.0010	114.854	0.283193	0.000010	16.99	0.37	16.2
z3	0.283191	0.000007	0.000010	0.0012	114.854	0.283188	0.000010	16.81	0.36	10.3
z4	0.283188	0.000003	0.000010	0.0014	114.854	0.283185	0.000010	16.70	0.35	41.1
z5	0.283190	0.000002	0.000010	0.0011	114.854	0.283188	0.000010	16.80	0.35	63.5
z6	0.283201	0.000004	0.000010	0.0008	114.854	0.283199	0.000010	17.21	0.37	22.9
z7	0.283192	0.000003	0.000010	0.0011	114.854	0.283190	0.000010	16.87	0.35	31.3
z8	0.283183	0.000005	0.000011	0.0013	114.854	0.283181	0.000011	16.54	0.38	14.6
<u>NF13 (9R-4 56-64)</u>										
z1	0.283195	0.000003	0.000010	0.0033	114.741	0.283188	0.000010	16.81	0.36	23.5
z2	0.283184	0.000003	0.000010	0.0044	114.741	0.283174	0.000010	16.32	0.35	61.6
<u>NF15 (9R-2 11-17)</u>										
z1	0.283198	0.000002	0.000008	0.0013	115.199	0.283196	0.000008	17.08	0.27	141.6
z3	0.283195	0.000002	0.000010	0.0012	115.199	0.283192	0.000010	16.97	0.35	78.7
z5	0.283206	0.000003	0.000010	0.0010	115.199	0.283203	0.000010	17.36	0.36	46.7
z6dil	0.283192	0.000002	0.000010	0.0013	115.199	0.283189	0.000010	16.86	0.35	99.0
z7	0.283193	0.000002	0.000010	0.0010	115.199	0.283191	0.000010	16.92	0.34	122.0
z9	0.283211	0.000001	0.000007	0.0018	115.199	0.283207	0.000007	17.50	0.27	204.8
<u>NF19 (9R-1 146-148)</u>										
z1	0.283203	0.000016	0.000019	0.0011	115.71	0.283201	0.000019	17.28	0.66	2.3
z2	0.283196	0.000010	0.000014	0.0012	115.71	0.283194	0.000014	17.03	0.50	3.8
<u>FC1</u>										
za	0.282184	0.000005	0.000010	0.0011	1099	0.282162	0.000010	2.60	0.34	11.6
zb	0.282171	0.000003	0.000008	0.0008	1099	0.282156	0.000008	2.38	0.30	52.2
zc	0.282173	0.000003	0.000008	0.0009	1099	0.282154	0.000008	2.32	0.30	75.0
zd	0.282187	0.000003	0.000009	0.0014	1099	0.282157	0.000009	2.44	0.31	51.5
ze	0.282179	0.000003	0.000008	0.0010	1099	0.282158	0.000008	2.46	0.30	48.0
zf	0.282179	0.000003	0.000008	0.0010	1099	0.282158	0.000008	2.46	0.30	53.0
<u>R33 (University of Arizona)</u>										
za	0.282751	0.000003	0.000008	0.0017	419	0.282737	0.000008	7.66	0.30	58.2
zb	0.282753	0.000003	0.000008	0.0015	419	0.282741	0.000008	7.79	0.30	52.3
zc	0.282751	0.000002	0.000008	0.0016	419	0.282738	0.000008	7.66	0.30	115.5
zd	0.282752	0.000003	0.000008	0.0018	419	0.282738	0.000008	7.67	0.30	49.8
ze	0.282746	0.000002	0.000008	0.0011	419	0.282738	0.000008	7.66	0.29	99.6
zf	0.282753	0.000002	0.000008	0.0013	419	0.282743	0.000008	7.85	0.30	64.9

91500											
zb	0.282308	0.000003	0.000008	0.0003	1063.6	0.282301	0.000008	6.74	0.28		34.3
zc	0.282301	0.000005	0.000009	0.0003	1063.6	0.282295	0.000009	6.53	0.31		16.2
zd	0.282304	0.000003	0.000008	0.0003	1063.6	0.282297	0.000008	6.60	0.28		41.9
ze	0.282306	0.000004	0.000008	0.0003	1063.6	0.282300	0.000008	6.69	0.29		28.5

* Modern $^{176}\text{Hf}/^{177}\text{Hf}$ ratios measured by MC-ICP-MS on purified Hf aliquots. See supplementary file with analytical methods for details
 † Internal uncertainties (2 SE) estimated for each individual run based on counting statistics
 § Total analysis uncertainty (2 SE) estimated from the propagation of individual internal uncertainties and 2 SD reproducibility of bracketing 25 ppb JMC-475 Hf standards used for correction. See supplementary file with analytical methods for details
 # $^{176}\text{Lu}/^{177}\text{Hf}$ compositions estimated from elemental Lu/Hf ratios measured on our 'trace element' aliquots and using a 'natural' $^{175}\text{Lu}/^{176}\text{Lu} = 0.02655$ from Vervoort et al. (2004). See supplementary file with analytical methods for details
 ** Initial $^{176}\text{Hf}/^{177}\text{Hf}$ ratios corrected for radiogenic ingrowth using the calculated $^{176}\text{Lu}/^{177}\text{Hf}$ composition of each zircon and the decay constant of Söderlund et al. (2004); $1.867 \times 10^{-11} \text{ yr}^{-1}$
 †† Uncertainty on the initial $^{176}\text{Hf}/^{177}\text{Hf}$ ratio assumed as the total uncertainty of the $^{176}\text{Hf}/^{177}\text{Hf}_{(0)}$ ratio. No uncertainties on the estimated $^{176}\text{Lu}/^{177}\text{Hf}$ or $\lambda^{176}\text{Lu}$ were propagated

TABLE DR4: $^{176}\text{Hf}/^{177}\text{Hf}$ ISOTOPIC COMPOSITION OF MORB BETWEEN THE AZORES AND CHARLIE GIBBS FRACTURE ZONE

Sample Name	Reference	Latitude	Longitude	$^{176}\text{Hf}/^{177}\text{Hf}$
TRI0154-019-003	Agranier et al. (2005)	40.74	-29.25	0.283359
TRI0154-018-002	Agranier et al. (2005)	41.18	-29.31	0.283269
TRI0154-017-002	Agranier et al. (2005)	41.67	-29.26	0.283252
TRI0154-016-003	Agranier et al. (2005)	42.39	-29.4	0.283233
TRI0154-015-002	Agranier et al. (2005)	42.79	-29.36	0.283173
AI0032-3-012-008	Agranier et al. (2005)	42.96	-29.18	0.283142
TRI0154-012-001	Agranier et al. (2005)	43.37	-28.98	0.283233
TRI0154-012-002	Agranier et al. (2005)	43.37	-28.98	0.28325
TRI0154-013-001	Agranier et al. (2005)	44.00	-28.39	0.283247
TRI0154-014-005	Agranier et al. (2005)	44.82	-28.04	0.283238
TRI0154-014-001	Kelley et al. (2013)	44.82	-28.04	0.283256
CHR0043-104-016	Agranier et al. (2005)	45.18	-27.9	0.283351
HUD1966-047-B1	Agranier et al. (2005)	45.37	-28.22	0.283229
TRI0138-001-002	Agranier et al. (2005)	46.23	-27.39	0.283254
TRI0138-002-003	Agranier et al. (2005)	47.05	-27.35	0.283273
TRI0138-003-001	Agranier et al. (2005)	47.78	-27.64	0.283248
TRI0138-005-001	Agranier et al. (2005)	49.52	-28.54	0.283246
TRI0138-006-001B	Andres et al. (2004)	50.043	-28.933	0.283429
TRI0138-007-001A	Blichert-Toft et al. (2005)	50.46	-29.42	0.283346
TRI0138-008-001	Blichert-Toft et al. (2005)	51.28	-30.02	0.283301
TRI0138-009-002	Blichert-Toft et al. (2005)	51.56	-29.92	0.283324
TRI0138-011-001	Blichert-Toft et al. (2005)	52.01	-29.95	0.283292

Mean is 0.28327 ± 0.00013 (2σ).